Nonionic Triblock and Star Diblock Copolymer and Oligomeric Surfactant Syntheses of Highly Ordered, Hydrothermally Stable, Mesoporous Silica Structures

Dongyuan Zhao,[†,‡] Qisheng Huo,[†,‡] Jianglin Feng,[‡] Bradley F. Chmelka,[‡,§] and Galen D. Stucky*[,†,‡]

Contribution from the Department of Chemistry, Materials Research Laboratory, and Department of Chemical Engineering. University of California, Santa Barbara, California 93106

Received November 25, 1997

Abstract: A family of highly ordered mesoporous (20−300 Å) silica structures have been synthesized by the use of commercially available nonionic alkyl poly(ethylene oxide) (PEO) oligomeric surfactants and poly(alkylene oxide) block copolymers in acid media. Periodic arrangements of mescoscopically ordered pores with cubic $Im\bar{3}m$, cubic $Pm\bar{3}m$ (or others), 3-d hexagonal ($P6_3/mmc$), 2-d hexagonal ($p6mm$), and lamellar (L_α) symmetries have been prepared. Under acidic conditions at room temperature, the nonionic oligomeric surfactants frequently form cubic or 3-d hexagonal mesoporous silica structures, while the nonionic triblock copolymers tend to form hexagonal ($p6mm$) mesoporous silica structures. A cubic mesoporous silica structure (SBA-11) with $Pm\bar{3}m$ diffraction symmetry has been synthesized in the presence of $C_{16}H_{33}(OCH_2CH_2)_{10}OH$ ($C_{16}EO_{10}$) surfactant species, while a 3-d hexagonal ($P6_3/mmc$) mesoporous silica structure (SBA-12) results when $C_{18}EO_{10}$ is used. Surfactants with short EO segments tend to form lamellar mesostructured silica at room temperature. Hexagonal mesoporous silica structures with d(100) spacings of 64−77 Å can be synthesized at 100 °C by using oligomeric nonionic surfactants. Highly ordered hexagonal mesoporous silica structures (SBA-15) with unusually large d(100) spacings of 104−320 Å have been synthesized in the presence of triblock poly(ethylene oxide)−poly(propylene oxide)−poly(ethylene oxide) (PEO−PPO−PEO) copolymers. SBA-15 mesoporous structures have been prepared with BET surface areas of 690−1040 m^2/g, pore sizes of 46−300 Å, silica wall thicknesses of 31−64 Å, and pore volumes as large as 2.5 cm^3/g. A novel cubic ($Im\bar{3}m$) cage-structured mesoporous silica structure (SBA-16) with a large cell parameter (a = 176 Å) has been synthesized using triblock copolymers with large PEO segments. The EO/PO ratio of the copolymers can be used to control the formation of the silica mesophase: lowering this ratio of the triblock copolymer moieties promotes the formation of lamellar mesostructured silica, while higher ratios favor cubic mesostructured silica. Cubic mesoporous structures are also obtained when star diblock copolymers are used as structure-directing agents. The calcined ordered mesoporous silicas reported in this paper are thermally stable in boiling water for at least 48 h. The assembly of the inorganic and organic periodic composite materials appears to take place by a hydrogen bonding ($S^0\ H^+)(X^-I^+$) pathway. The assembly rate r increases with increasing concentration of [H^+] and [Cl^-], according to the kinetic expression $r = k[H^+]^{0.31}[Cl^-]^{0.31}$.

Introduction

Nonionic alkyl poly(oxyethylene) surfactants and poly(oxyalkylene) block copolymers are important families of surfactants that are widely used in emulsifying, defoaming/antifoaming, coating, thickening, solubilizing, cleaning, lubricating, wetting, pharmaceutical,[1] coal and petrochemical industries, and household applications.[2−4] They display excellent interfacial stabilization properties and are low-cost, nontoxic, and biodegradable.

In composite materials synthesis, nonionic block copolymers are an interesting class of structure-directing agents whose self-assembly characteristics lead to kinetically quenched structures. Block copolymers have the advantage that their ordering properties can be nearly continuously tuned by adjusting solvent composition, molecular weight, or copolymer architecture. Moreover, they permit solution organization of larger structural features than is possible with low-molecular-weight surfactants, and they achieve this from lower solution concentrations. Novel morphologies and material properties can be produced by exploiting kinetically hindered microdomain separations in such systems, using as a guide insight on the existence and sequence of mesoscopic morphologies obtained in closely related copolymer/homopolymer blends.[5] Close analogies also exist in strictly organic systems, in which heterogeneous nanoscale structures have been controllably produced and stabilized as block copolymer composites containing polymerizable additives.

[†] Department of Chemistry.
[‡] Materials Research Laboratory.
[§] Department of Chemical Engineering.

(1) Schmolka, I. R. In *Polymers for Controlled Drug Delivery*; Tarcha, P. J., Ed.; CRC Press: Boston, 1991; Chapter 10.

(2) Chu, B.; Zhou, Z. In *Nonionic Surfactants: Polyoxyalkylene Block Copolymers*; Nace, V. M., Ed.; Surface Science Series Vol. 60; Marcel Dekker: New York, 1996.

(3) Sjöblom, J.; Stenius, P.; Danielsson, I. In *Nonionic Surfactants: Physical Chemistry*; Nace, V. M., Ed.; Surface Science Series Vol. 23; Marcel Dekker: New York, 1987.

(4) Meziani, A.; Tourand, D.; Zradba, A.; Pulvin, S.; Pezron, I.; Clausse, M.; Kunz, W. *J. Phys. Chem. B* **1997**, *101*, 3620.

(5) Matsen, M. W. *Macromolecules* **1995**, *28*, 5765. Matsen, M. W.; Schick, M. *Curr. Opin. Colloid Interface Sci.* **1996**, *1*, 329.

S0002-7863(97)04025-0 CCC: $15.00 © 1998 American Chemical Society
Published on Web 06/09/1998

An excellent example of this is the work of Hillmyer et al. in which they selectively incorporated and cross-linked a thermosetting epoxy resin in the PEO domains of a poly(ethylene oxide)−poly(ethylethylene) (PEO−PEE) diblock copolymer.[6]

The overall strategy of using block copolymers in materials synthesis is thus applicable not only to composites containing hydrophilic−hydrophobic copolymers, such as the silica−poly(alkylene oxide) system,[7] but more generally to any self-assembling surfactant or copolymer system in which a network-forming additive is selectively partitioned among different mesostructured components. An enormous variety of nanophase-separated composite materials can be envisioned in which variations in the choice of blocks, copolymer compositions, solvents, or chain architecture are used to tune self-assembly, while processing variables such as temperature, pH, aligning fields, etc., are manipulated to regulate fixation of the resultant structure(s).

Pinnavaia and co-workers[8,9] used nonionic surfactants in aqueous solutions to synthesize wormlike disordered mesoporous silica and alumina in neutral media assembled by hydrogen-bonding interactions.[8−10] Attard et al.[11] have synthesized hexagonal mesoporous silica phases using concentrated (∼50 wt %) $C_{12}EO_8$ solutions and suggested that the formation of mesoporous silica under these conditions occurs by a "real" liquid crystal template route. It should be noted, however, that the methanol produced by hydrolysis of tetramethyl orthosilicate (TMOS) initially destroys the liquid crystalline order formed by the surfactant. This, along with the varying concentration of water during the hydrolysis of TMOS and condensation of silica species under acid synthesis conditions, make the preservation of the liquid crystalline order throughout the composite assembly process questionable.[12,13]

Templin et al.[14] have used high concentrations of poly(isoprene-*b*-ethylene oxide) diblock copolymers (PI-*b*-PEO) to make lamellar and hexagonal aluminosilicate−polymer mesostructures that are highly ordered on length scales to ∼40 nm. The syntheses were carried out in an acidic and nonaqueous solution (a mixture of $CHCl_3$ and tetrahydrofuran). The thermal stability of these materials and removal of the organic phase to create mesoporous structures has not yet been described.

Mesoporous silica materials organized with nonionic surfactant species that display periodic structural order and that are made under neutral or basic synthesis conditions have not yet been reported. Of considerable interest in this regard is the report by Voegtlin et al.[15] of the synthesis of ordered mesoporous silica that gives an improved X-ray diffraction pattern by using nonionic surfactants in the presence of fluoride anions under near-neutral conditions. They postulate that the F^- ions are coordinated to silica intermediates, $S^0H^+(F^-I^0)$, which apparently provide sufficient electrostatic shielding and effective hydrogen bonding to form mesoporous silica structures that yield relatively narrow (100) Bragg diffraction peaks (full width at half-maximum (fwhm) = 0.15−0.5 with Cu Kα radiation).

For several reasons, including product cost, environmental, and biomimetic considerations, we have sought to use dilute aqueous organic concentrations in silica composite and mesoporous materials syntheses. Built into this has been the idea of cooperative self-assembly[16−18] of the molecular inorganic and organic species, which together influence the final morphology and mesoscopic ordering obtained and both of which can be controlled kinetically and via inorganic−organic interface interactions.

Consistent with the results of Voegtlin et al.[15] and our earlier studies,[17−19] balanced Coulombic, hydrogen bonding, and van der Waals interactions with charge matching in aqueous syntheses provide an effective means of enhancing long-range periodic order. Such interactions are particularly important at the inorganic−organic interface and can be realized by working with cationic silica species below the aqueous isoelectric point of silica (pH ∼2). With cationic surfactants and syntheses carried out in HCl media below the aqueous isoelectric point of silica, the key interactions are among the cationic surfactant, chloride anion, and the cationic silica species (designated as $S^+X^-I^+$, where S^+ is the cationic surfactant, X^- is the halide anion, and I^+ is a protonated Si−OH moiety, i.e., $[SiO^H_H]^+$, and the overall charge balance is provided by association with an additional halide anion).[19,20]

Solubilization of nonionic poly(alkylene oxide) surfactants and block copolymers in aqueous media is due to the association of water molecules with the alkylene oxide moieties through hydrogen bonding.[2] This should be enhanced in acid media where hydronium ions, instead of water molecules, are associated with the alkylene oxygen atoms, thus adding long-range Coulombic interactions to the coassembly process. If carried out below the aqueous isoelectric point of silica, cationic silica species will be present as precursors, and the assembly might be expected to proceed through an intermediate of the form $(S^0H^+)(X^-I^+)$. The anion may be coordinated directly to the silicon atom through expansion of the silicon atom's coordination sphere. Our goal in this research was to use this structure-directing route to create highly ordered structures with low-cost, nontoxic, and biodegradable nonionic organics under relatively dilute aqueous conditions. In particular, we chose to investigate the use of block copolymers in order to extend the range and control of inorganic−organic mesophase structures from nanometer to larger length scales.[7]

Here we report new mesoporous silica structures that include cubic ($Im\bar{3}m$ and $Pm\bar{3}m$), three-dimensional hexagonal ($P6_3/mmc$), two-dimensional hexagonal ($p6mm$), possibly continuous L_3 sponge and lamellar (L_α) mesostructures synthesized by using low molecular weight nonionic ethylene oxide surfactants and poly(alkylene oxide) block copolymers in acid media via an $(S^0H^+)(X^-I^+)$ synthesis route.[21,22] Under these conditions, our results show that the structure of ordered mesoporous silica

(6) Hillmyer, M.; Lipic, P. M.; Hajduk, D. A.; Almdal, K.; Bates, F. S. *J. Am. Chem. Soc.* **1997**, *119*, 2749.
(7) Zhao, D.; Feng, J.; Huo, Q.; Melosh, N.; Fredrickson, G. H.; Chmelka, B. F.; Stucky, G. D. *Science* **1998**, *279*, 548.
(8) Bagshaw, S. A.; Prouzet, E.; Pinnavaia, T. J. *Science* **1995**, *269*, 1242.
(9) Bagshaw, S. A.; Pinnavaia, T. J. *Angew. Chem., Int. Ed. Engl.* **1996**, *35*, 1102.
(10) Prouzet, E.; Pinnavaia, T. J. *Angew. Chem., Int. Ed. Engl*. **1997**, *36*, 516.
(11) Attard, G. S.; Glyde, J. C.; Göltner, C. G. *Nature* **1995**, *378*, 366.
(12) Göltner, C. G.; Antonietti, M. *Adv. Mater.* **1997**, *9*, 431.
(13) Antonietti, M.; Göltner, C. *Angew. Chem., Int. Ed. Engl*. **1997**, *36*, 910.
(14) Templin, M.; Franck, A.; Chesne, A. D.; Leist, H.; Zgang, Y.; Ulrich, R.; Schädler, U.; Wiesner, U: *Science* **1997**, *278*, 1795.
(15) Voegtlin, A. C.; Ruch, F.; Guth, J. L.; Patarin, J.; Huve, L. *Microporous Mater*. **1997**, *9*, 95.
(16) Monnier, A.; Schüth, F.; Huo, Q.; Kumar, D.; Margolese, D.; Maxwell, R. S.; Stucky, G. D.; Krishnamurty, M.; Petroff, P.; Firouzi, A.; Janicke, M.; Chmelka, B. F. *Science* **1993**, *261*, 1299.
(17) Firouzi, A.; Kumar, D.; Bull, L. M.; Besier, T.; Sieger, P.; Huo, Q.; Walker, S. A.; Zasadzinski, J. A.; Glinka, C.; Nicol, J.; Margolese, D.; Stucky, G. D.; Chmelka, B. F. *Science* **1995** *267*, 1138.
(18) Firouzi, A.; Atef, F.; Oertli, A. G.; Stucky, G. D.; Chmelka, B. F. *J. Am. Chem. Soc*. **1997**, *119*, 3596.
(19) Huo, Q.; Margolese, D. I.; Stucky, G. D. *Chem. Mater*. **1996**, *8*, 1147.
(20) Huo, Q.; Margolese, D. I.; Ciesia, Feng, P.; Gier, T. E.; Sieger, P.; Leon, R.; Petroff, P. M.; Schüth, F.; Stucky, G. D. *Nature* **1994**, *368*, 317.
(21) Mercier, L.; Pinnavaia, T. J. *Adv. Mater*. **1997**, *9*, 500.
(22) Braun, P. V.; Osenar, P.; Stupp, S. I. *Nature* **1996**, *380*, 325.

is controlled predominantly by the surfactant species selected and that each type of surfactant favors formation of a specific mesostructured silica phase. Under the reaction conditions used here, nonionic oligomeric ethylene oxide surfactants often result in the formation of cubic phases, while triblock copolymers tend to yield hexagonal mesostructures at room temperature. X-ray diffraction, nitrogen adsorption/desorption isotherms, and transmission electron micrograph (TEM) data show that the mesoporous silica products are highly ordered, with BET surface areas up to 1160 m^2/g. Importantly, after calcination the mesoporous products are thermally stable even in boiling water. High-quality hexagonal mesoporous silica (*p6mm*) synthesized by this approach has a much larger cell parameter (a = 120−320 Å), a larger uniform pore size (47−300 Å), a larger pore volume (up to 2.5 cm^3/g), and thicker silica walls (31−64 Å) than MCM-41 synthesized by using conventional low-molecular weight cationic surfactants.

Experimental Section

Chemicals. All surfactants are commercially available from Aldrich, Fluka, and BASF and were used as received, including the following: Brij 52, $C_{16}H_{33}(OCH_2CH_2)_2OH$, designated $C_{16}EO_2$, (Aldrich); Brij 30, $C_{12}EO_4$, (Aldrich); Brij 56, $C_{16}EO_{10}$, (Aldrich); Brij 58, $C_{16}EO_{20}$, (Aldrich); Brij 76, $C_{18}EO_{10}$, (Aldrich); Brij 78, $C_{16}EO_{20}$, (Aldrich); Brij 97, $C_{18}H_{35}EO_{10}$, (Aldrich); Brij 35, $C_{12}EO_{23}$, (Aldrich); Triton X-100, $CH_3C(CH_3)_2CH_2C(CH_3)_2C_6H_4(OCH_2CH_2)_xOH$, x = 10 (av), (Aldrich); Triton X-114, $CH_3C(CH_3)_2CH_2C(CH_3)_2C_6H_4(OCH_2CH_2)_5OH$ (Aldrich); Tween 20, poly(ethylene oxide) (20) sorbitan monolaurate (Aldrich); Tween 40, poly(ethylene oxide) (20) sorbitan monopalmitate (Aldrich); Tween 60, poly(ethylene oxide) (20) sorbitan monostearate (Aldrich); Tween 80, poly(ethylene oxide) (20) sorbitan monooleate (Aldrich); and Span 40, sorbitan monopalmitate (Aldrich). The structures are as follows:

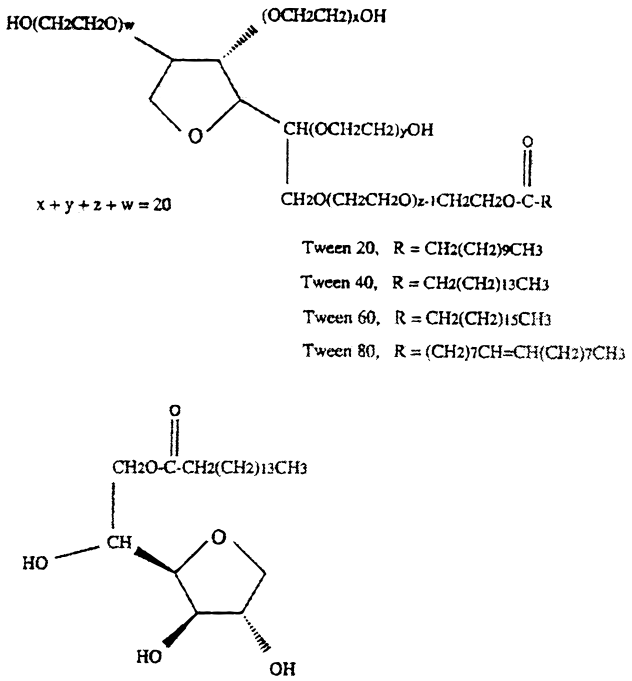

Span 40 Sorbitan monopalmitate

Other surfactants used include Tergitol TMN 6, $CH_3CH(CH_3)CH(CH_3)CH_2CH_2CH(CH_3)(OCH_2CH_2)_6OH$ (Fulka); Tergitol TMN 10, $CH_3CH(CH_3)CH(CH_3)CH_2CH_2CH(CH_3)(OCH_2CH_2)_{10}OH$ (Fulka); block copolymers having a poly(ethylene oxide)−poly(propylene oxide)−poly(ethylene oxide) (EO−PO−EO) sequence centered on a (hydrophobic) poly(propylene glycol) nucleus terminated by two primary hydroxyl groups; Pluronic L121 (M_{av} = 4400), $EO_5PO_{70}EO_5$ (BASF); Pluronic L64 (M_{av} = 2900), $EO_{13}PO_{30}EO_{13}$ (BASF); Pluronic P65 (M_{av} = 3400), $EO_{20}PO_{30}EO_{20}$ (BASF); Pluronic P85 (M_{av} = 4600), $EO_{26}PO_{39}EO_{26}$ (BASF); Pluronic P103 (M_{av} = 4950), $EO_{17}PO_{56}EO_{17}$ (BASF); Pluronic P123 (M_{av} = 5800), $EO_{20}PO_{70}EO_{20}$, (Aldrich); Pluronic F68 (M_{av} = 8400), $EO_{80}PO_{30}EO_{80}$ (BASF); Pluronic F127 (M_{av} = 12 600), $EO_{106}PO_{70}EO_{106}$ (BASF): Pluronic F88 (M_{av} = 11 400), $EO_{100}PO_{39}EO_{100}$ (BASF); Pluronic 25R4 (M_{av} = 3600), $PO_{19}EO_{33}PO_{19}$ (BASF); star diblock copolymers having four EO_n-PO_m chains (or in reverse, the four PO_n-EO_m chains) attached to an ethylenediamine nucleus, and terminated by secondary hydroxyl groups; Tetronic 908 (M_{av} = 25 000), $(EO_{113}PO_{22})_2$ $NCH_2CH_2N(PO_{113}EO_{22})_2$ (BASF); Tetronic 901 (M_{av} = 4700), $(EO_3PO_{18})_2$ $NCH_2CH_2N(PO_{18}EO_3)_2$ (BASF); and Tetronic 90R4 (M_{av} = 7240), $(PO_{19}EO_{16})_2$ $NCH_2CH_2N(EO_{16}PO_{19})_2$ (BASF). Tetraethoxysilane (TEOS) (Aldrich), tetramethoxysilane (TMOS) (Aldrich), and tetrapropoxysiliane (TPOS) (Aldrich) were used as silica sources.

Syntheses. Mesoporous silica phases were synthesized at room temperature (RT) by using nonionic surfactants as the structure-directing agents. In a typical preparation, 4.0 g of Brij 76 was dissolved in 20 g of water and 80 g of 2 M HCl solution with stirring. Then 8.80 g of TEOS was added to that homogeneous solution with stirring at room temperature for 20 h. The solid product was recovered, washed, and air-dried at room temperature. Yields are typically ∼95% (based on silicon), which is similar to that obtained using low-molecular weight cationic surfactant species under acid conditions.[19,20]

Silica−block copolymer mesophases were synthesized by this procedure at 35−60 °C, except the synthesis using Pluronic F127 which was reacted at room temperature. In a typical preparation, 4.0 g of Pluronic P123 was dissolved in 30 g of water and 120 g of 2 M HCl solution with stirring at 35 °C. Then 8.50 g of TEOS was added into that solution with stirring at 35 °C for 20 h. The mixture was aged at 80 °C overnight without stirring. The solid product was recovered, washed, and air-dried at RT. Yields are ∼98% (based on silicon), which is comparable to the syntheses described above. Calcination was carried out by slowly increasing temperature from room temperature to 500 °C in 8 h and heating at 500 °C for 6 h.

Analyses. X-ray powder diffraction (XRD) patterns were taken on a Scintag PADX diffractometer equipped with a liquid nitrogen cooled germanium solid-state detector using Cu Kα radiation. The nitrogen adsorption and desorption isotherms at 77 K were measured using a Micromeritics ASAP 2000 system. The sample was pretreated at 200 °C overnight in the vacuum line. The data were analyzed by the BJH (Barrett−Joyner−Halenda) method using the Halsey equation for multilayer thickness. The pore size distribution curve came from the analysis of the adsorption branch of the isotherm. The pore volume was taken at the P/P_0 = 0.985 single point. High-resolution ^{29}Si MAS NMR spectra were recorded on a Chemagnetics CMX-500 spectrometer operating at a ^{29}Si resonance frequency of 59.71 MHz under conditions of magic-angle spinning at 3 kHz at room temperature; $\pi/2$ pulse lengths of 6−7 μs were used to acquire one-pulse ^{29}Si spectra resulting from 100−300 signal-averaged accumulations, employing a 300 s repetition delay between each scan. The ^{29}Si MAS spectra are referenced to tetramethylsilane, $Si(CH_3)_4$. Transmission electron micrographs (TEM) were taken on a 2000 JEOL electron microscope operating at 200 kV. The samples for TEM were prepared by dispersing a large number of particles of the products through a slurry in acetone onto a holey carbon film on a Ni grid. A Netzsch Thermoanalyzer STA 409 was used for simultaneous thermal analysis combining thermogravimetry (TG), derivative thermogravity (DTG), and difference thermoanalysis (DTA) with a heating rate of 5 K min^{-1} in air.

Results and Discussion

1. Oligomeric Alkyl−Ethylene Oxide Surfactants. (a) $C_{16}EO_{10}$ Surfactant. The powder XRD pattern (Figure 1 (bottom)) of as-synthesized mesoporous silica SBA-11 prepared in the presence of oligomeric nonionic surfactant species $C_{16}EO_{10}$ shows evidence of three reflections at 2θ values between 1 and 2° (one strong peak and two shoulder peaks) with d spacings of ∼56.6 Å. Calcination at 500 °C for 6 h yields a

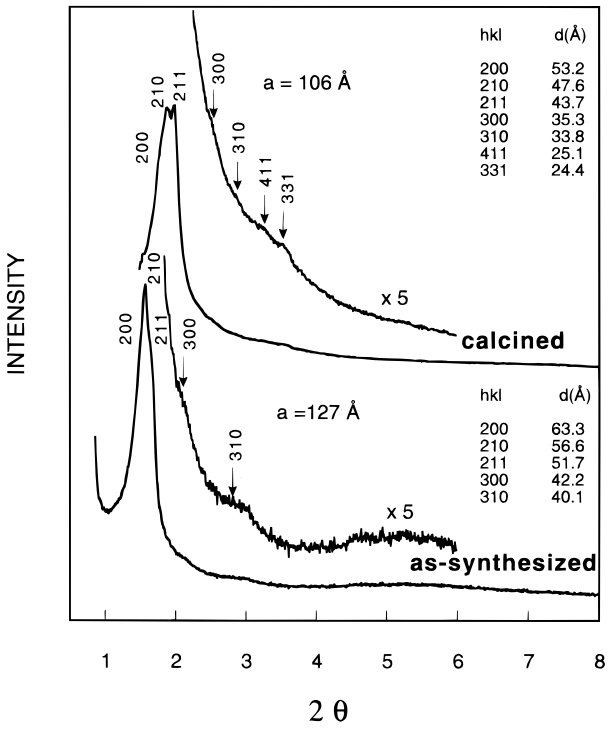

Figure 1. Powder X-ray diffraction patterns of the cubic mesoporous silica structure SBA-11 prepared by using $C_{16}EO_{10}$ surfactant species at room temperature.

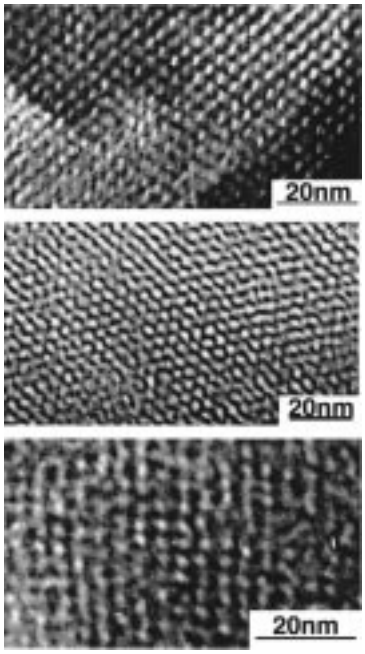

Figure 2. Transmission electron micrographs with different orientations (top, [110]; middle, [111]; bottom, [001]) of calcined cubic mesoporous silica SBA-11 prepared by using $C_{16}EO_{10}$ surfactant species at room temperature.

better-resolved XRD pattern (Figure 1 (top)), in which a third shoulder peak is observed with a slight decrease of *d* values, as expected.[19,20,23−25] In addition, two new peaks are resolved at 2θ values between 3 and 4°. After calcination, the intensities of the XRD peaks are substantially greater than those measured from the as-synthesized products, suggesting that SBA-11 is stable and the siloxane condensation promoted during the calcination process improves the long-range mesoscopic ordering of the pores. The XRD patterns of as-synthesized SBA-11 can be indexed as a cubic mesophase belonging to the $Pm\bar{3}m$ (221) space group (or others such as $P23$ (195), $Pm\bar{3}$ (200), $P432$ (207), $P\bar{4}32$ (215)). Use of $C_{16}EO_{10}$ as structure-directing species yields products with unit cell parameters (*a*) of 127 and 106 Å for as-synthesized and calcined SBA-11, respectively. Further evidence for a cubic mesostructure is provided by the TEM images presented in Figure 2, which are representative of mesoporous silica prepared with $C_{16}EO_{10}$. The micrograph shows well-ordered mesopore structures viewed along the [111], [011], and [001] directions, suggesting that the mesoporous silica is a highly ordered three-dimensional cubic mesostructure.

The binary phase diagrams of nonionic surfactants, such as $C_{16}EO_8$ and $C_{16}EO_{12}$, in water contain cubic (I), hexagonal (H_1), cubic (V_1), and lamellar (L_α, L_2) phases, respectively, with increasing surfactant concentration.[3,26,27] In addition, two cubic phases have been reported at relatively low surfactant concentrations (I_1' and I_1'').[28,29] One of these structures is $Pm\bar{3}n$, which is the same as that found by Mitchell et al., while the other is different but not clearly defined.[28,29] A cubic $Pm\bar{3}m$ (diffraction symmetry) or possibly distorted cubic mesostructured silica film made by using cationic ($C_{16}H_{33}N(CH_3)_3Br$, CTAB) surfactant species under acidic conditions has recently been observed by Brinker and co-workers.[30] The results here suggest that the $C_{16}EO_{10}$ surfactant species yield a cubic $Pm\bar{3}m$ mesoporous silica phase under the acid synthesis conditions used.

The N_2 adsorption−desorption isotherm (Figure 3 (main plot) for SBA-11 is type IV without hysteresis[31,32] and shows a well-defined step in the adsorption and desorption curve between partial pressures P/P_0 of 0.2−0.4. Such adsorption behavior is indicative of the filling of framework-confined mesopores with an average BJH pore size of 25 Å.[32−34] The fwhm of 5 Å measured for the pore-size distribution (Figure 3, inset) indicates that SBA-11 has well-defined uniform pore dimensions. It is similar to that observed for mesoporous silica prepared with surfactant species containing an alkylammonium head group (5 Å).[19,32] The pore-size distribution is narrower than that of the wormlike disordered materials produced by S^0I^0 templating using nonionic surfactant species under neutral conditions (9 Å).[8−10] Calcined SBA-11 has a N_2 BET surface area of 1070 m^2/g and a pore volume of 0.68 cm^3/g (Table 1).

Thermogravimetic (TGA) and differential thermal (DTA) analyses of SBA-11 show three weight loss steps in the TGA curve, with a total weight loss of 55 wt %, and one endothermic

(23) Kresge, C. T.; Leonowicz, M. E.; Roth, W. J.; Vartuli, J. C.; Beck, J. S. *Nature* **1992**, *359*, 710.
(24) Beck, J. S.; Vartuli, J. C.; Roth, W. J.; Leonowicz, M. E.; Kresge, C. T.; Schmitt, K. T.; Chu, C. T.-W.; Olson, D. H.; Sheppard, E. W.; McCullen, S. B.; Higgins, J. B.; Schlenker, J. L. *J. Am. Chem. Soc*. **1992**, *114*, 10834.
(25) Huo, Q.; Leon, R.; Petroff, P. M.; Stucky, G. D. *Science* **1995**, *268*, 1324.
(26) Mitchell, D. J.; Tiddy, G. J. T.; Waring, L.; Bostock, T.; McDonald, M. P. *J. Chem. Soc., Faraday Trans. 1* **1983**, *79*, 975.
(27) Danino, D.; Talmon, Y.; Zana, R. *J. Colloid Interface Sci.* **1997**, *186*, 170.
(28) Jahns, E.; Finkelmann, H. *Colloid. Polym. Sci.* **1987**, *265*, 304.
(29) Funari, S.; Rapp, G. *J. Phys. Chem. B* **1997**, *101*, 732.
(30) Lu, Y.; Ganguli, R.; Drewien, C. A.; Anderson, M. T.; Brinker, J. C.; Gong, W.; Guo, Y.; Soyez, H.; Dunn, B.; Huang, M. H.; Zink, J. I. *Nature* **1997**, *389*, 364.
(31) Sing, K. S. W.; Everett, D. H.; Haul, R. A. W.; Moscou, L.; Pierotti, R. A.; Rouquérol, J.; Siemieniewska, T. *Pure Appl. Chem*. **1985**, *57*, 603.
(32) Schmidt, R.; Hansen, E. W.; Stöcker, M.; Akporiaye, D.; Ellestad, O. H. *J. Am. Chem. Soc.* **1995**, *117*, 4049.
(33) Branton, P. J.; Hall, P. G.; Sing, K. S. W.; Reichert, H.; Schüth, F.; Unger, K. K. *J. Chem. Soc., Faraday Trans*. **1994**, *90*, 2965.
(34) Llewellyn, P. L.; Grillet, Y.; Schüth, F.; Reichert, H.; Unger, K. K. *Microporous Mater*. **1994**, *3*, 345.

Table 1. Physicochemical Properties of Mesoporous Silica (SBA) Prepared Using Nonionic Alkyl Poly(ethylene oxide) Surfactants

surfactant	reaction temp	mesophase	d^a (Å)	BET surface area (m^2/g)	pore size^b (Å)	pore vol (cm^3/g)
$C_{16}EO_2$	RT	lamellar	64.3			
$C_{12}EO_4$	RT	cubic	45.3 (44.7)	670	22	0.38
$C_{12}EO_4$	RT	lamellar	45.7	570		
$C_{12}EO_4$	60 °C	L_3 (?)	42.4	610	24	0.39
$C_{16}EO_{10}$	RT	cubic	56.6 (47.6)	1070	25	0.68
$C_{16}EO_{10}$	100 °C	hexagonal	64.1 (62.8)	910	35	1.02
$C_{16}EO_{20}$	RT	cubic	63.7 (49.6)	600	22	0.29
$C_{18}EO_{10}$	RT	$P6_3/mmc$	63.5 (51.0)	1150	31	0.83
$C_{18}EO_{10}$	100 °C	hexagonal	77.4 (77.0)	910	40	0.92
$C_{18}H_{35}EO_{10}$	RT	$P6_3/mmc$	49.1 (47.7)	1000	27	0.59
$C_{12}EO_{23}$	RT	cubic	54.8 (43.3)	500	16	0.24
Tween 20	RT	cubic	55.1 (46.8)	800	19	0.37
Tween 40	RT	cubic	52.4 (49.6)	700	20	0.36
Tween 60	RT	cubic	63.8 (53.9)	720	24	0.52
Tween 60	RT	lamellar	38.7			
Tween 80	RT	cubic	62.2 (53.9)	710	25	0.43
Span 40	RT	lamellar	55.5			
Triton X100	RT	cubic	41.8 (35.5)	780	17	0.35
Triton X114	RT	cubic	42.2 (36.7)	990	16	0.45
Teritor TMN 6	RT	cubic	44.3 (39.9)	1160	23	0.57
Teritor TMN 10	RT	cubic	42.3 (36.5)	800	20	0.38

^{a} d(100) spacing or d value of characteristic reflection of the as-synthesized products; the number inside brackets is the d value after calcination at 500 °C for 6 h. ^{b} Calculated from adsorption branch.

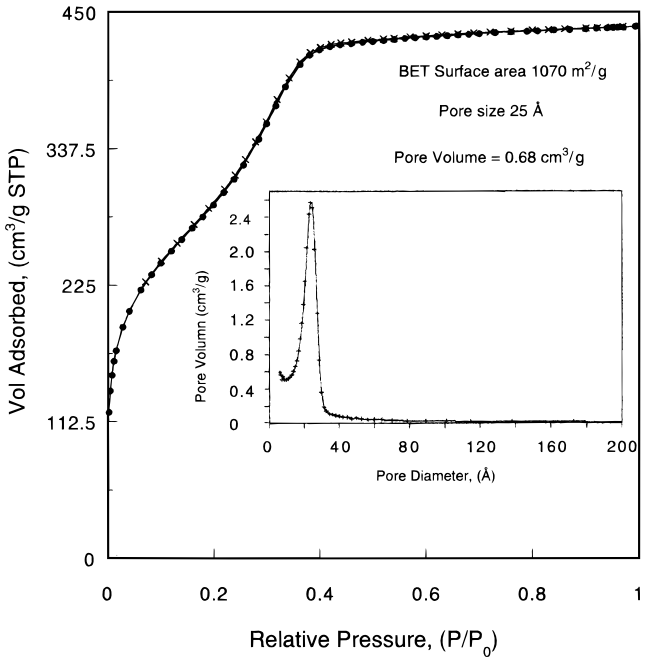

Figure 3. Nitrogen adsorption−desorption isotherm plots and pore size distribution curve from the adsorption branch of calcined cubic (*Pm*3*m*) mesoporous silica SBA-11 prepared by using $C_{16}EO_{10}$ surfactant species at room temperature.

and two exothermic peaks in the DTA curve. The endothermic loss near 80 °C (7 wt % loss) is assigned to water desorption,[35,36] whereas the exothermic weight losses at 210 °C (25 wt % loss) and 310 °C (23 wt % loss) are assigned to desorption and decomposition of surfactant species.[35,36] By 320 °C, essentially all of the nonionic organic surfactant species have been removed from the SBA-11 channels, which occurs at a much lower temperature than that (∼460 °C) needed for removal of the cationic surfactant agents such as CTAB used under basic conditions to prepare MCM-41 mesoporous silica.[35,36] This is consistent with the weaker interactions expected between the nonionic surfactant and inorganic silica wall, compared to that of cationic CTAB with silica under basic MCM-41 synthesis conditions. The thicker silica walls observed for materials prepared with PEO−PPO−PEO species[7] are thought to result from a combination of such weaker PEO−silica interactions and the weaker microphase-separating tendency of PEO−PPO, relative to the MCM-41 system.

The solid-state one-pulse ^{29}Si MAS NMR spectrum (see Supporting Information Figure I) of as-synthesized SBA-11 prepared at RT shows three broad peaks at 92, 99, and 109 ppm, corresponding to Q^2, Q^3, and Q^4 silica species, respectively. The ratio Q^3/Q^4 is about 0.92, suggesting incomplete silica condensation, while the broad peaks are consistent with a locally disordered silica framework.

SBA-11 can be synthesized over a wide composition range (1:0.036−0.6:0.4−20:97−650 TEOS:$C_{16}EO_{10}$:HCl:H_2O) at RT. TMOS and TPOS can also be used as sources of silica. The mesophase symmetry is not changed by varying the surfactant-to-silica ratio (<0.6) at RT, and only cubic SBA-11 is formed. At higher surfactant/silica ratios (>0.6), a poorly ordered unstable lamellar-like mesophase is formed, possibly because the $C_{16}EO_{10}$ is not completely dissolved. Lower surfactant/silica ratios (<0.036) induce only partial precipitation of the silica species. The results indicate that at RT, the $C_{16}EO_{10}$ surfactant favors a cubic mesophase. At higher temperatures, a hexagonal mesoporous silica structure (*p*6*mm*) is formed, consistent with molecular packing considerations.[17,37] Figure 4 shows the XRD patterns of as-synthesized and calcined hexagonal mesoporous silica prepared using the same composition as that for cubic SBA-11 (1:0.144:2:85 TEOS:$C_{16}EO_{10}$:HCl:H_2O), but after 20 h of reaction at RT and subsequent heating at 100 °C without stirring for 3 days. This mesostructured silica synthesized at a higher temperature (100 °C) shows three well-defined peaks at 2θ values between 1 and 8° (Figure 4) that can be indexed as (100), (110), and (200) Bragg reflections, typical of hexagonal (*p*6*mm*) SBA-15, mesoporous silica.[7] This material is thermally stable after calcination at 500 °C, as evidenced by retention of

(35) Huo, Q.; Margolese, D. I.; Ciesla, U.; Demuth, D. G.; Feng, P.; Gier, T. E.; Sieger, P.; Firouzi, A.; Chmelka, B. F.; Schüth, F.; Stucky, G. D. *Chem. Mater.* **1994**, *6*, 1176.

(36) Chen, C.; Li, H.; Davis, M. E. *Microporous Mater.* **1993**, *2*, 17.

(37) Israelachvili, J. N. In *Physics of Amphiphiles: Micelles, Vesicles and Microemulsions*; Societa Italiana di Fisica; Bologna, Italy, 1985; pp 24−58.

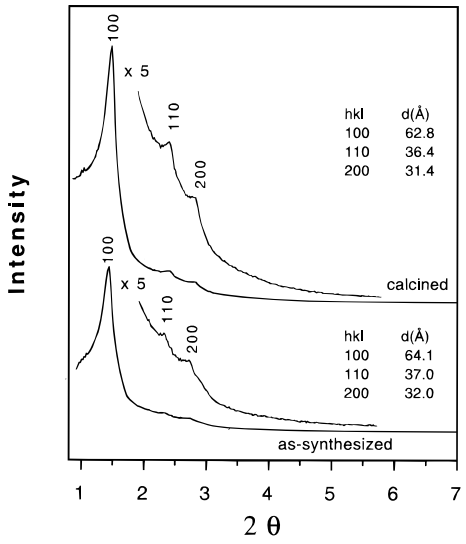

Figure 4. Powder X-ray diffraction patterns of as-synthesized and calcined *p*6*mm* hexagonal mesoporous silica (SBA-15) prepared by using $C_{16}EO_{10}$ surfactant species at 100 °C for 3 days.

a well-resolved hexagonal XRD pattern (Figure 4), which reflects a unit cell parameter of $a = 72.5$ Å.

The results suggest that hexagonal SBA-15 mesoporous silica can be formed using $C_{16}EO_{10}$ species only at higher temperatures (100 °C), consistent with the appearance of the hexagonal mesophase at higher temperatures (50−80 °C) for the binary $C_{16}EO_{10}$−water system.[3,26] The N_2 adsorption and desorption isotherms of hexagonal mesoporous silica are of type IV and show a uniform mean pore size of 35 Å (fwhm = 5 Å).[31] The BET surface area and pore volume of the calcined materials are 910 and 1.02 cm^3/g, respectively (Table 1). The approximate pore size calculated by the BJH formula is much smaller than the repeat distance ($a = d(100) \times 2/\sqrt{3} = 72.5$ Å) determined by XRD, the latter of which also includes the thickness of the silica walls. Thus, we estimate that the pore wall of the hexagonal mesoporous silica prepared using the $C_{16}EO_{10}$ surfactant species is about 38 Å thick, substantially thicker than the wall of the *p*6*mm* phase prepared using cationic quaternary ammonium surfactants for MCM-41 under basic conditions (10−15 Å)[23,24,36] or SBA-3 under acidic conditions (15−20 Å).[20,35]

(b) $C_{18}EO_{10}$ Surfactant. Figure 5 shows the XRD patterns of as-synthesized and calcined mesoporous silica SBA-12 prepared in the presence of $C_{18}EO_{10}$ surfactant species. For as-synthesized SBA-12, three poorly resolved peaks appear in the 2θ range of 1−2° with *d* spacings of 65.7, 63.5, and 58.3 Å, and two weak but resolved peaks in the 2θ range of 2−5° with *d* spacings of 24.4 and 21.8 Å (Figure 5a). With longer reaction times, two unresolved additional reflections with *d* spacings of 38.2 and 35.5 Å may be present (Figure 5b). After calcination at 500 °C, these peaks are still observed, though they appear at higher angles, consistent with slight contraction of the framework.[19,20,23−25,36] The XRD patterns of SBA-12 (Figure 5) can be indexed in the space group $P6_3/mmc$ with unit cell parameters $a = 76.5$, $c = 127$ Å for as-synthesized SBA-12, with $c/a = 1.66$. After calcination, the unit cell of the sample ($a = 63.4$ Å, $c = 102$ Å, $c/a = 1.61$) contracts 10−25 Å.[19,25] TEM images (Figure 6) show a regular array of mesopores for different orientations [0001] (top), $[1\bar{2}\bar{1}3]$ (middle), and $[01\bar{1}1]$ (bottom) and further confirm that SBA-12 has $P6_3/mmc$ space group symmetry and a three-dimensional hexagonal structure.[25]

The N_2 adsorption−desorption isotherm (see Supporting Information Figure II) of three-dimensional hexagonal SBA-12 is of type IV with a small H_1 hysteresis loop[31,32] and shows a well-defined step in the curve at a normalized partial pressure P/P_0 of 0.2−0.5. The pore-size distribution determined by using a BJH analysis shows a narrow peak (fwhm = 5 Å) and a mean pore size of 31 Å. The BET surface area and pore volume of SBA-12 are measured to be 1150 m^2/g and 0.83 cm^3/g, respectively. The results indicate that SBA-12 has a uniform monodisperse mesopore size.[31,32]

We have previously reported that three-dimensional hexagonal ($P6_3/mmc$) mesoporous silica (SBA-2) can be synthesized by the use of gemini surfactants, such as $[C_{18}H_{37}N(CH_3)_2(CH_2)_3N(CH_3)_3]Br_2$ (designated C_{18-3-1}).[19,25] The C_{n-s-1} surfactants have high charge densities and large effective head groups, which favor globular aggregate structures[38] and the formation of the three-dimensional $P6_3/mmc$ hexagonal mesophase. The nonionic $(EO)_{10}$ moiety of $C_{18}EO_{10}$ appears to behave analogously to the large head groups of quaternary ammonium cationic surfactant species,[25,39] and induces formation of the $P6_3/mmc$ hexagonal mesostructured SBA-12. Compared to SBA-2 (which has a three-dimensional hexagonal $P6_3/mmc$ structure prepared by using a gemini surfactant), the XRD patterns of SBA-12 show poorly resolved peaks in the 2θ range of 2−8°, but the ratio of $d(002)$ to $d(112)$ of 1.91 is close to that (1.90) of SBA-2.[19,25] In addition, we have examined the structure with TEM and confirmed that SBA-12 prepared with $C_{18}EO_{10}$ has the same mesostructure as SBA-2, albeit with a much larger unit cell ($a = 75.8$, $c = 127$ Å). The appearance of a $P6_3/mmc$ mesophase is consistent with simple molecular packing considerations and the effective packing parameter $g = V/a_0l$, where V is the total volume of the surfactant chain plus a contribution from any cosolvent organic molecules present, a_0 is the effective head group area at the micelle surface, and l is the kinetic surfactant tail length.[39] In comparing $C_{16}EO_{10}$ and $C_{18}EO_{10}$, both surfactants have similar EO_{10} head groups and comparable molecular volumes, but the chain length in $C_{18}EO_{10}$ is slightly longer, which is expected to lead to structures with greater curvature. In other words, the shorter kinetic surfactant tail length of $C_{16}EO_{10}$ produces a larger g value than that for $C_{18}EO_{10}$, consistent with the latter's formation of more curved aggregates arranged in a three-dimensional hexagonal structure.[19,25]

The TGA and DTA curves for 3-d hexagonal SBA-12 are similar to those for cubic SBA-11, but the total weight loss is ∼45 wt %; 39 wt % of the total weight loss is attributed to decomposition of the organic species. These weight changes are less than for SBA-11 (55 wt %, 48 wt %) and indicate that as-synthesized SBA-12 contains less total concentration of the structure-directing surfactant species.

Like SBA-11, SBA-12 can be synthesized at room temperature over a wide range of compositions (1:0.03−0.5:0.4−20:97−650 TEOS:$C_{18}EO_{10}$:HCl:H_2O). If the surfactant-to-silica ratio is varied at RT, the three-dimensional hexagonal $P6_3/mmc$ mesophase is retained. By increasing the temperature (to 100 °C), SBA-12 can be transformed from the 3-d hexagonal symmetry ($P6_3/mmc$) to the plane group hexagonal (*p*6*mm*) mesoporous silica structure (Table 1).

(c) Tween-Type Surfactant. Mesoporous silica can be synthesized by the use of alkyl−EO/furan surfactants, such as Tween 20, 40, 60, 80 (structure shown in the Experimental

(38) Hagslatt, H.; Soderman, O.; Jonsson, B. *Langmuir* **1994**, *10*, 2177.
(39) Israelachvili, J. N.; Mitchell, D. J.; Ninham, B. W.; *J. Chem. Soc., Faraday Trans. 2* **1976**, *72*, 1525; *Biochim. Biophys. Acta* **1977**, *470*, 185.

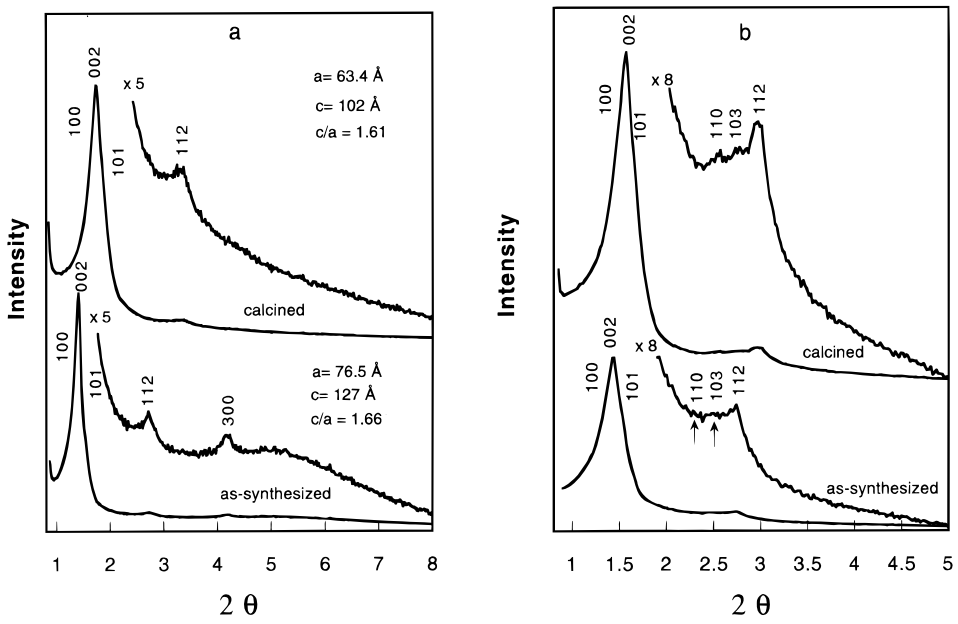

Figure 5. Powder X-ray diffraction patterns of 3-d hexagonal ($P6_3/mmc$) SBA-12 prepared by using $C_{18}EO_{10}$ surfactant species at room temperature for (a 1 day and (b 4 days.

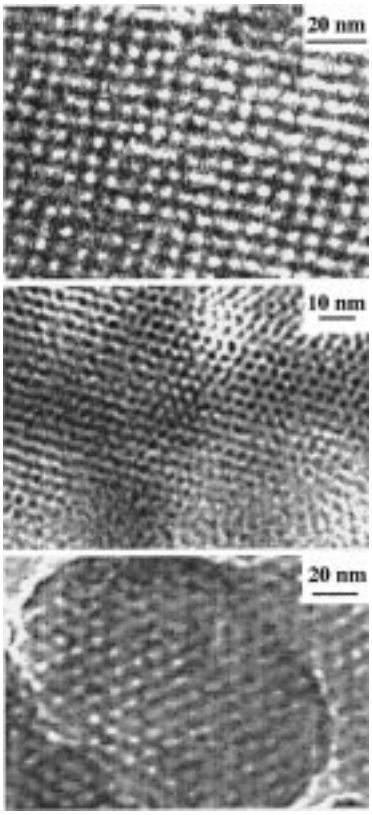

Figure 6. Transmission electron micrographs with different orientations top, [0001]; middle, [$1\bar{2}1\bar{3}$]; and bottom, [$01\bar{1}1$]) of calcined 3-d hexagonal ($P6_3/mmc$) SBA-12 prepared by using $C_{18}EO_{10}$ surfactant species at room temperature.

Section). Such materials prepared at lower concentrations of the surfactant (e.g., 0.5 wt %) (see Supporting Information Figure III) show only one narrow peak, with a *d* spacing of ~64 Å, in the XRD pattern, independent of the Tween surfactant used. At higher concentrations of surfactant, another peak with a *d* spacing of ~40 Å appears, along with its higher-order reflections. The intensities of these peaks increase with increasing concentration of surfactant, so that when the concentration of the surfactant is higher than 16 wt %, a lamellar mesostructure with a well-resolved XRD pattern is obtained (see Supporting Information Figures III and IV). This is accompanied by disappearance of the peak at 64 Å at higher concentrations of Tween surfactant.

The XRD patterns (see, for example, Supporting Information Figure IV) of the lamellar mesostructured silica formed with Tween surfactant concentrations greater than 16% are well-resolved. The (400) and (500) reflections are also observed at higher scattering angles. TGA data of the lamellar mesostructured silica show a total weight loss of 91 wt %, with 11 wt % coming from adsorbed water and 80 wt % from decomposition of the surfactant, indicating that this lamellar mesostructured silica contains only about 9 wt % silica and 80 wt % surfactant. This corresponds approximately to one molecular surfactant species interacting on average with four to five molecular siloxane or silica species. This lamellar mesostructured silica is unstable to calcination at 500 °C for 6 h.

For the less-well-defined mesostructural silica prepared at low concentrations of Tween surfactant, calcination at 500 °C for 6 h yields a mesoporous product. Thus, mesoporous silica prepared, for example, using Tween 60 surfactant had a BET surface area of 720 m^2/g. Like those of SBA-11 and SBA-12, its N_2 adsorption and desorption isotherm is type IV with a narrow BJH pore size distribution centered at 24 Å (fwhm = 6 Å) (Table 1). TEM images following calcination (not shown) indicate that this mesoporous silica has a unique three-dimensional cubic mesostructure; the data at this time are not adequate to determine the specific space group.

As shown in Table 1, mesoporous silica structures can also be synthesized by using Tween 20, 40, and 80 as structure-directing agents; the first two are shorter-chain surfactants than Tween 60. The mesophase structure of the products is the same for these surfactant species, independent of their EO moiety lengths. Also the BET surface areas and *d* spacings (Table 1) are independent of the EO moiety lengths for the Tween surfactants, even though the pore sizes do increase slightly with the length of the EO segments. This illustrates the manner in

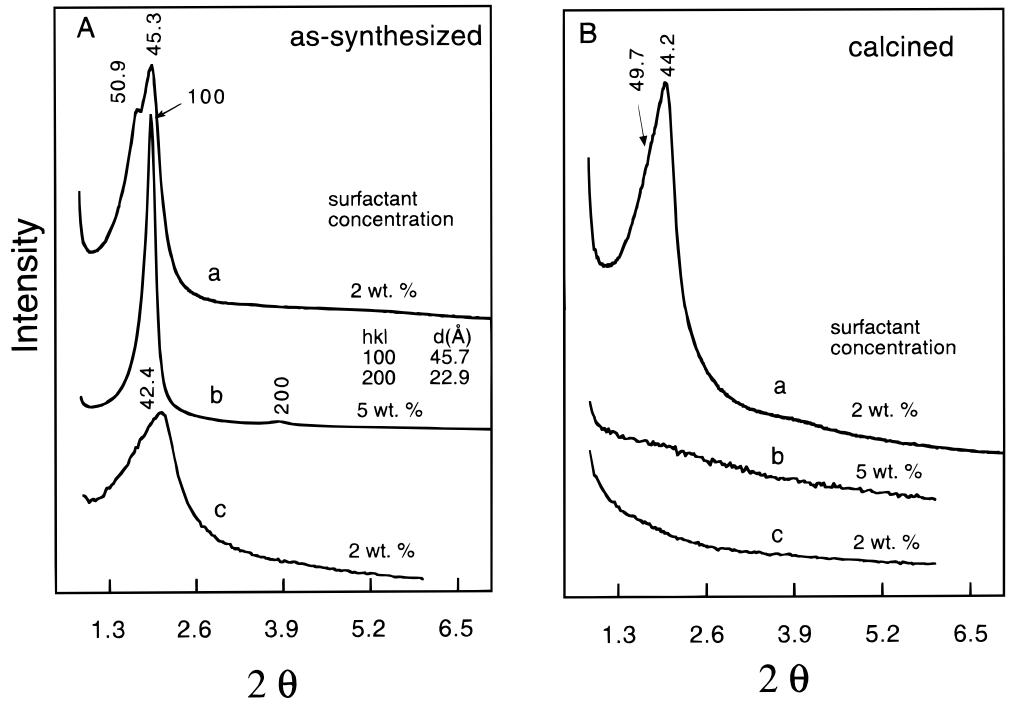

Figure 7. Powder X-ray diffraction patterns of (A) as-synthesized and (B) calcined mesoporous silicas prepared by using $C_{12}EO_4$ surfactant species with different concentrations and reaction temperatures.

which hydrophobic/hydrophilic interactions can be used to control pore dimensions and periodicities.

When Span 40 (sorbitan monopalmitate), which has a structure similar to Tween 40 but without the EO/furan moiety is used as a structure-directing agent, only lamellar mesostructured silica is obtained with $d(100) \sim 55.5$ Å. This suggests that in the absence of EO moiety head groups, there are weaker interactions between the surfactant species and silica cations, leading to aggregate lower interfacial curvatures, and lamellar mesostructures.

(d) $C_{12}EO_4$ Surfactant. Ordered mesoporous silica can also be synthesized at low surfactant concentrations at room temperature by using oligomeric nonionic surfactants with short EO segments, such as $C_{12}EO_4$. Figure 7 shows the XRD patterns of as-synthesized and calcined mesostructured silica prepared with varying concentrations of $C_{12}EO_4$ surfactant species at different reaction temperatures. At RT and a low concentration of surfactant (<3 wt %), a stable mesoporous silica (SBA-14) is formed. As shown in Figure 7A (pattern a), the XRD pattern of as-synthesized SBA-14 shows two peaks at *d* spacing of 50.9 and 45.3 Å. After calcination, the first peak becomes poorly resolved, while the second remains clearly observed with a small decrease (0.5 Å) in *d* spacing (Figure 7B, pattern a). Calcined SBA-14 has a type-IV N_2 adsorption/desorption isotherm (see Supporting Information Figure Va) with a mean narrow pore size of 22 Å (fwhm = 5.5 Å). The BET surface area of these SBA-14 materials is 670 m^2/g (see Table 1). Although in most regions of the phase diagram of the binary water−$C_{12}EO_4$ system the surfactant forms lamellar mesophases, cubic mesophases are observed at low temperature (−2 °C). A cubic $Pm\bar{3}n$ mesophase has also been observed in the $C_{12}EO_2$ surfactant−water system at RT by Funari and Rapp.[29] The two peaks in the XRD pattern of SBA-14 have a *d* spacing ratio of 1.12, which is close to the ratio $\sqrt{5}/\sqrt{4} = 1.118$ and consequently consistent with a cubic structure for SBA-14. TEM images also indicate that SBA-14 has a three-dimensional cubic structure. With higher concentrations of surfactant (>5%), only lamellar mesostructured silica (L_α) with $d(100) \sim 45.7$ Å is formed (Figure 7A, pattern b). As shown in Figure 7B, all XRD reflections are lost after calcination at 500 °C, suggesting that the lamellar mesostructured silica (L_α) collapses.[19,23,24]

SBA-14 that is thermally stable during calcination is synthesized under ambient temperature conditions. When the reaction temperature is increased to 60 °C, an as-synthesized material is produced with a broad X-ray diffraction peak at a *d* spacing of 42.4 Å. As shown in Figure 7A, pattern c, this silica product has a broad peak at low scattering intensity, which is quite different from the lamellar mesostructured silica (Figure 7A, pattern b). After calcination at 500 °C diffraction peaks are not observed (Figure 7B, pattern c), suggesting that the partially ordered structures collapse. However, the N_2 adsorption/desorption isotherm (see Supporting Information Figure Vb) of this calcined material is type IV with an H_2 hysteresis loop; it shows a defined step in the adsorption and desorption curves between partial pressures P/P_0 of 0.2−0.4, along with a low peak in the BJH pore-size distribution (from the adsorption branch), corresponding to a pore size of 24 Å (fwhm = 6 Å). These results are quite different from those for lamellar mesostructured silica (L_α) (see Supporting Information Figure Vc), the isotherms of which do not show step or hysteresis loops; no pores in the mesoscopic size range are observed in the BJH pore-size distribution curve. TEM images of the material represented in Figure 7A, pattern c, show a homogeneous disordered mesostructure that is similar to that found for an L_3 sponge structure previously reported by McGrath et al.[40] Mitchell et al.[3,26] have pointed out that the $C_{12}EO_4$ surfactant in low concentrations in a binary water−surfactant system can form the L_3 sponge phase at 50−80 °C. McGrath et al. used a cationic surfactant (cetylpyridinium chloride) to synthesize a sponge silicate L_3 phase also under acidic conditions.[40] Therefore, the L_3 structure may be reasonable for the silica product prepared at 60 °C using low concentrations of $C_{12}EO_4$, though more extensive investigations are required to confirm this.

(40) McGrath, K. M.; Dabbs, D. M.; Yao, N.; Aksay, I. A.; Gruner, S. M. *Science* **1997**, *277*, 552.

Table 2. Physicochemical Properties of Mesoporous Silica (SBA) Prepared Using Poly(alkylene oxide) Triblock Copolymers

block copolymer	formula	mesophase	d^a (Å)	BET surface area (m^2/g)	pore size[b] (Å)	pore vol (cm^3/g)	wall thickness[c] (Å)
Pluronic L121	$EO_5PO_{70}EO_5$	lamellar	116				
Pluronic L121	$EO_5PO_{70}EO_5$	hexagonal	118 (117)	630	100	1.04	35
Pluronic F127	$EO_{106}PO_{70}EO_{106}$	cubic	124 (118)	740	54	0.45	
Pluronic F88	$EO_{100}PO_{39}EO_{100}$	cubic	118 (101)	700	35	0.36	
Pluronic F68	$EO_{80}PO_{30}EO_{80}$	cubic	91.6 (88.9)				
Pluronic P123	$EO_{20}PO_{70}EO_{20}$	hexagonal	104 (95.7)	690	47	0.56	64
Pluronic P123	$EO_{20}PO_{70}EO_{20}$	hexagonal	105 (97.5)*[d]	780	60	0.80	53
Pluronic P123	$EO_{20}PO_{70}EO_{20}$	hexagonal	103 (99.5)*[e]	820	77	1.03	38
Pluronic P123	$EO_{20}PO_{70}EO_{20}$	hexagonal	108 (105)*[f]	920	85	1.23	36
Pluronic P123	$EO_{20}PO_{70}EO_{20}$	hexagonal	105 (104)*[g]	850	89	1.17	31
Pluronic P103	$EO_{17}PO_{85}EO_{17}$	hexagonal	97.5 (80.6)	770	46	0.70	47
Pluronic P65	$EO_{20}PO_{30}EO_{20}$	hexagonal	77.6 (77.6)	1000	51	1.26	39
Pluronic P85	$EO_{26}PO_{39}EO_{26}$	hexagonal	92.6 (88.2)	960	60	1.08	42
Pluronic L64	$EO_{13}PO_{70}EO_{13}$	hexagonal	80.6 (80.5)	950	59	1.19	34
Pluronic 25R4	$PO_{19}EO_{33}PO_{19}$	hexagonal	74.5 (71.1)	1040	48	1.15	34
Tetronic 908		cubic	101 (93.6)	1050	30	0.69	
Tetronic 901		cubic	73.9 (70.1)				
Tetronic 90R4		cubic	7.39 (68.5)	1020	45	0.91	

[a] $d(100)$ spacing or d value of characteristic reflection of the as-synthesized products; the value inside brackets is the d value after calcination at 500 °C for 6 h. [b] Calculated from adsorption branch of the N_2 isotherm. [c] Calculated by a_0 − pore size ($a_0 = 2d(100)/\sqrt{3}$). *Reaction at 35 °C for 20 h, then heating: (d) at 80 °C for 24 h; (e) at 80 °C for 48 h; (f) at 90 °C for 24 h; (g) at 100 °C for 24 h.

Table 1 summarizes the physicochemical properties of SBA mesoporous silica structures prepared under acidic conditions using different ethylene oxide-based surfactants with different lengths of hydrophobic alkyl chains or EO segments. The length of the EO moieties has a strong effect on the structure of the silica mesophase that is formed. Surfactant species containing shorter EO segments, such as $C_{16}EO_2$, form lamellar mesostructured silica, while those containing longer EO blocks, such as $C_{16}EO_{20}$ and $C_{12}EO_{23}$, can be used to form cubic mesoporous silica, though at low surfactant concentrations (<2 wt %). Higher concentrations result in no precipitation of silica or the formation of silica gel. The BET surface areas and d spacing values for these products do not appear to be closely related to the lengths of the alkyl chains or the EO segments.

2. Poly(alkylene oxide) Block Copolymers. SBA-15. Ordered mesoporous silica structures can also be synthesized using poly(alkylene oxide) triblock copolymer surfactant species. The X-ray pattern of as-synthesized SBA-15 prepared using $EO_{20}PO_{70}EO_{20}$ (Pluronic P123) (see Supporting Information Figure VIa) shows four well-resolved peaks that can be indexed as (100), (110), (200), and (210) diffraction peaks associated with *p*6*mm* hexagonal symmetry. Three additional peaks appear in the 2θ range of 2.5−3.5° that can be indexed as (300), (220), and (310) scattering reflections, respectively.[7] The intense (100) peak reflects a d spacing of 104 Å, corresponding to a large unit cell parameter (a = 120 Å). After calcination in air at 500 °C for 6 h, the XRD pattern contains peaks at somewhat higher scattering angles, $d(100)$ = 95.7 Å, for which a cell parameter a of 110 Å is established. Six peaks are still observed, confirming that hexagonal SBA-15 is thermally stable. TEM images (see Supporting Information Figure VII) of calcined SBA-15 at different orientations confirm that SBA-15 has a two-dimensional *p*6*mm* hexagonal structure, with a well-ordered hexagonal array and one-dimensional channel structure.[7] The average distance between mesopores is about 110 Å, in agreement with that determined from the XRD data. A similarly high degree of mesoscopic order is reflected by the XRD pattern (not shown) of hexagonal SBA-15 even after calcination to 850 °C.

SEM images reveal that as-synthesized SBA-15 has a wheatlike macroscopic particle morphology with uniform mean sizes of about 80 μm and that these consist of many ropelike aggregates.[7] Calcined SBA-15 shows a similar particle morphology, reflecting the thermal stability of the macroscopic structure. Calcined SBA-15 prepared with the $EO_{20}PO_{70}EO_{20}$ triblock copolymer surfactant species at 35 °C has a pore size of 47 Å, a pore volume of 0.56 cm^3/g, and a BET surface area of 690 m^2/g (see Supporting Information Figure VIIIa). Three well-distinguished regions of the adsorption isotherm from calcined SBA-15 are noticed: monolayer−multilayer adsorption, capillary condensation, and multilayer adsorption on the outer surface of SBA-15. In contrast to the N_2 adsorption results[32,33] for ordered mesoporous silica MCM-41 with mean pore sizes of less than 40 Å, a clear type-H_2 small hysteresis loop in the adsorption−desorption isotherm of SBA-15 is observed and the capillary condensation occurs at higher relative pressures. From the $d(100)$ spacing and the mean pore size determined by N_2 adsorption, the estimated mean thickness of the pore walls of hexagonal siliceous SBA-15 prepared by using $EO_{20}PO_{70}EO_{20}$ surfactant species is about 64 Å. This is substantially thicker than the walls of MCM-41 silica prepared by using amphiphilic alkylammonium ion surfactants as structure-directing species.

Heating as-synthesized SBA-15 in the reaction solution at different temperatures (80−140 °C) and for different lengths of time (11−72 h) results in a systematic series of structures (see Supporting Information Figure VIIIb and Table 2) with different pore sizes (47−89 Å) and different silica wall thicknesses (31−64 Å). The average pore sizes determined from the TEM images are slightly less than those from N_2 adsorption measurements, while the wall thicknesses from TEM images are somewhat larger than those calculated from X-ray and N_2 adsorption measurements. The walls are, in general, substantially thicker than those typical for MCM-41 (commonly ∼10−15 Å) prepared using alkylammonium ion surfactant species for structural organization.[23,24,36] Higher temperatures or longer reaction times result in larger pore sizes and thinner silica walls. The large pore sizes and silica wall thicknesses may be caused by the relatively long hydrophilic EO blocks of the copolymer. In acid solution the hydrophilic EO moieties are expected to interact with the protonated silica by the $(S^0H^+)(X^-I^+)$ mechanism described below and thus be closely associated with the inorganic wall.[20] Increasing the temperature results in increased hydrophobicity of the EO block moiety[41] and therefore decreases, on average, the lengths of the EO segments that are associated with the silica wall (see below). This tends to

(41) Zana, R. *Colloids Surf., A* **1997**, *123*−*124*, 27.

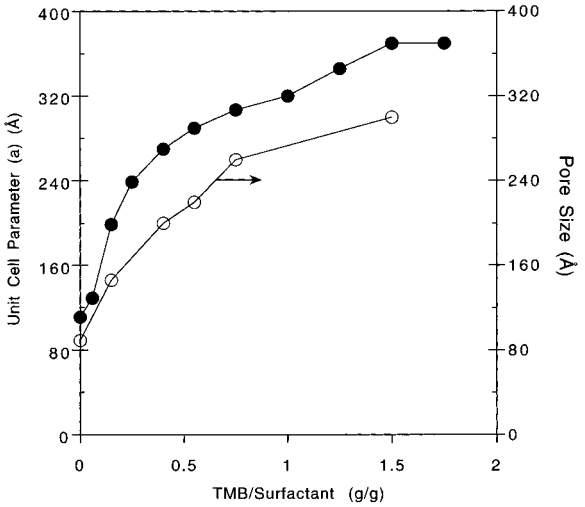

Figure 8. Variation of the unit cell parameter *a* (solid circles) and pore size (open circle) for calcined SBA-15 as a function of the TMB: surfactant ratio (g/g) (TMB = 1,3,5-trimethylbenzene). The pore sizes of the calcined SBA-15 were measured from the adsorption branch of the N_2 adsorption−desorption isotherm curve by the BJH method. The chemical compositions of the reaction mixture for the SBA-15 were 4 g of copolymer: *x* g:0.41 mol:0.24 mol:6.67 mol TMB:TEOS:HCl:H_2O.

increase the hydrophobic volumes of the surfactant aggregates, resulting in the increased pore sizes in SBA-15 materials prepared at higher temperatures (80 °C).

The pore size of hexagonal mesoporous SBA-15 can be expanded to ∼300 Å by the addition of cosolvent organic molecules, such as 1,3,5-trimethylbenzene (TMB). A typical X-ray pattern (see Supporting Information Figure VIb) of as-synthesized SBA-15 prepared by adding TMB as an organic swelling agent shows three resolved peaks with *d* spacings of 270, 154, and 133 Å at very low scattering angles (2θ range of 0.2−1°), which are indexable as (100), (110), and (200) reflections associated with *p*6*mm* hexagonal symmetry. The (210) reflection is too broad to be observed. The intense (100) peak reflects a *d* spacing of 270 Å, corresponding to an unusually large unit cell parameter (a = 310 Å). After calcination in air at 500 °C for 6 h, the XRD pattern becomes better resolved and a broad (210) reflection with a *d* spacing of 100 Å is additionally observed. These results confirm that hexagonal SBA-15 with a large lattice parameter is thermally stable and mesoscopically well-ordered. The N_2 adsorption−desorption results (see Supporting Information Figure VIIIc) show that the calcined product has a BET surface area of 910 m^2/g, a mean pore size of 260 Å, and a pore volume of 2.2 cm^3/g. TEM images confirm that the calcined products have highly ordered, hexagonal symmetry with large uniform pore sizes.

Control over the pore size of highly ordered hexagonal SBA-15 can be achieved over the range 89−300 Å (as measured by N_2 adsorption) by changing the amount of TMB cosolvent in the reaction mixture. As the TMB/copolymer weight ratio increases (the ratio in this study ranged from 0 to 2), the unit cell parameter *a* and pore size increase substantially and can reach 370 and 300 Å, respectively, under the conditions and mixture compositions used here (Figure 8). With this increase in cell parameter *a* and pore size, the hexagonal mesostructure is retained: the X-ray diffraction pattern of each material exhibits three to four peaks related by hexagonal symmetry. To the best of our knowledge, SBA-15 currently has the largest pore dimensions for periodic-structured mesoporous materials. The *d*(100) spacing and pore size of MCM-41 prepared by using cationic surfactant species can also be enlarged,[20,24] but the increase is much less than that for SBA-15.[7] On the other hand, although the pore size of MCM-41 can be expanded to 100 Å by adding auxiliary organic TMB, the XRD pattern consists of at most one peak for these materials (up to ∼100 Å pore size),[24] reflecting diminished mesoscopic ordering. The SBA-15 pore sizes determined by TEM images are slightly less than those obtained from N_2 adsorption measurements.

^{29}Si MAS NMR spectra (see Supporting Information Figure Ib) of as-synthesized SBA-15 show three peaks at Q^2 (92 ppm), Q^3 (99 ppm), and Q^4 (109 ppm). The ratio Q^3/Q^4 of 0.78 is lower than that (0.92) of SBA-11 prepared by using $C_{16}EO_{10}$ surfactant species, implying that the silica walls of SBA-15 are more highly condensed than they are in as-synthesized SBA-11. This may be caused by the higher reaction temperature (35 °C) used for SBA-15 than that for SBA-11 (25 °C, RT). The broad peaks in the ^{29}Si MAS NMR spectra show that SBA-15 has a locally disordered silica framework like that of MCM-41.

TGA and DTA analyses (see Supporting Information Figure IX) of SBA-15 prepared using $EO_{20}PO_{70}EO_{20}$ show a total weight loss of 58 wt %. The thermal analysis data show two processes: at intermediate temperature (80 °C), TGA shows a 12 wt % loss, accompanied by an endothermic DTA peak due to desorption of water, followed at higher temperature (145 °C) by a 46 wt % weight loss with an exothermic DTA peak due to decomposition of the organic copolymer species.[35,36]

The decomposition temperature (∼150 °C) of the PEO−PPO−PEO block copolymer species in SBA-15 is much lower than that of cationic CTA^+ surfactants in MCM-41 (∼360 °C).[35,36] As a result the organic copolymer species can be completely removed by heating SBA-15 in air at 140 °C for 3 h. This is also substantially lower than the decomposition temperature of alkyl nonionic surfactants, such as $C_{16}EO_{10}$ (∼210 °C). The pure block copolymer $EO_{20}PO_{70}EO_{20}$ decomposes at ∼250 °C. For comparison, the TGA of the copolymer $EO_{20}PO_{70}EO_{20}$ impregnated in SiO_2 gel shows that the copolymer can be decomposed and desorbed at 190 °C, which is ∼50 °C higher than necessary for SBA-15. While the copolymer species are not strongly bound to the silica pore walls, their removal from as-synthesized SBA-15 nevertheless occurs at a relatively low temperature (140 °C), suggesting a catalytic decomposition process.

An alternative method of removing the copolymer surfactant species is by low-temperature reflux in ethanol. Solvent extraction of as-synthesized SBA-15 allows the poly(alkylene oxide) triblock copolymer to be removed without decomposition, permitting its recovery and reuse (recovery yield, ∼95%). We have used such recycled copolymer species to synthesize highly ordered hexagonal SBA-15 (six XRD peaks were observed) with characteristics and properties that are identical to those presented above.

Under acidic conditions and temperatures from 35 to 80 °C, SBA-15 can be synthesized over a relatively narrow range of PEO−PPO−PEO copolymer concentrations (2−6 wt %). Higher concentrations of the block copolymer species form only silica gel or yield no precipitation of silica product; at lower concentrations, only amorphous silica is obtained. A reaction temperature of 35−80 °C is necessary for SBA-15 synthesis. At RT, only amorphous silica or poorly ordered products result, while higher temperatures (>80 °C) yield silica gel.

SBA-16. Novel mesoporous silica SBA-16 has been synthesized by using a poly(alkylene oxide) triblock copolymer, $EO_{106}PO_{70}EO_{106}$, with large EO blocks at room temperature.

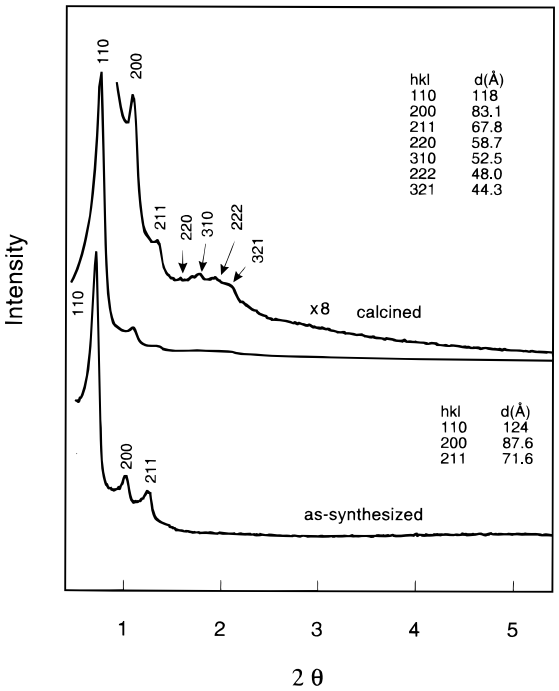

Figure 9. Powder X-ray diffraction patterns of as-synthesized and calcined $Im\bar{3}m$ cubic SBA-16 prepared by using poly(alkylene oxide) block copolymer $EO_{106}PO_{70}EO_{106}$ surfactant species at room temperature.

The XRD pattern (Figure 9) of as-synthesized SBA-16 shows a strong reflection with a large *d* spacing of 124 Å, two strong reflections in the 2θ range of 1−1.4° with *d* spacings of 87.6 and 71.6 Å, and several weaker reflections at 2θ values of 1.4−2.4°. After calcination at 500 °C in air for 6 h, these diffraction peaks are still observed though with *d* spacings reduced by 5−7 Å; in addition, the weak peaks at $2\theta = 1.4-2.4°$ become better resolved. The XRD pattern of SBA-16 can be indexed as (110), (200), (211), (220), (310), (222), (321) reflections corresponding to a cubic structure ($Im\bar{3}m$ space group, $a = 176$ or 166 Å for as-synthesized and calcined SBA-16, respectively). High-resolution TEM images of calcined SBA-16 with different orientations ([110], [111] planes; see Supporting Information Figure X) are consistent with a three-dimensional cubic cage structure with an ultralarge cell parameter. We have previously reported that cubic SBA-1 with $Pm\bar{3}n$ structure can be synthesized in the presence of cationic surfactant species with large head groups (such as alkyltriethylammonium) in acidic media.[20] The $EO_{106}PO_{70}EO_{106}$ triblock copolymer has a large molecular weight ($M_{av} = 12\,600$) and large EO moieties, which favor globular aggregate structures.[2,42] Only cubic (V_1) (∼15−70 wt %) and isotropic phases were observed for the Pluronic F127−water system at room temperature.[2,42] The copolymer $EO_{106}PO_{70}EO_{106}$ yields an $Ia\bar{3}d$ phase in a surfactant−water binary system and an $Im\bar{3}m$ silica mesophase under our synthesis conditions. The cubic $Im\bar{3}m$ mesophase has been observed in a ganglioside surfactant−water binary system[43−45] and poly(butylene oxide)-*b*-poly(ethylene oxide) diblock copolymer−water systems.[46] The cage structure of SBA-16 with its large cell parameter has potential advantages for catalysis and separation applications.

SBA-16 can be synthesized under acidic conditions over a narrow range of dilute $EO_{106}PO_{70}EO_{106}$ surfactant concentrations (3−5%) at room temperature. After reacting at RT for 20 h, high-quality SBA-16 was produced by heating the solid precipitate in the mother solution at 80 °C for 2 days. Higher copolymer concentrations result in the formation of silica gel, while lower concentrations lead to the formation of amorphous silica. As in the case of SBA-15, the triblock copolymer species can easily be removed from SBA-16 by low-temperature reflux in ethanol or by heating in air at 140 °C for 3 h. The TGA curve for SBA-16 shows a total weight loss of 46 wt %, with 11 wt % from water and 35 wt % from the organic block copolymer. Calcined SBA-16 has a pore size of 54 Å, a pore volume of 0.45 cm^3/g, and a BET surface area of 740 m^2/g. The N_2 adsorption−desorption isotherm (see Supporting Information Figure XI) is type IV with a type-H_1 hysteresis loop.[31] These results are consistent with a large-pore structure for the SBA-16.

Other Structures. A series of ordered mesoporous silica structures with different *d* spacings and pore sizes have been synthesized by using poly(alkylene oxide) triblock copolymers with different EO to PO ratios. Table 2 summarizes the physicochemical properties of mesoporous silica structures prepared by using triblock and star diblock copolymers with different architectures. Generally, these block copolymers favor formation of hexagonal mesoporous silica SBA-15 with *d*(100) spacings of 74.5−118 Å for as-synthesized SBA-15 without the addition of organic swelling agents. The EO-to-PO ratio and polymer architecture have a large effect on the formation of the mesostructured silica. Ratios of EO/PO = 0.07−1.5 favor the formation of hexagonal (*p6mm*) mesoporous silica structures. Lower ratios (<0.07) (for example, $EO_5PO_{70}EO_5$) at low concentrations (0.5−1 wt %) form hexagonal mesoporous silica SBA-15 and at higher concentrations (2−5 wt %) form lamellar mesostructured silica with a *d*(100) spacing of 116 Å. Higher EO/PO ratios (>1.5), e.g. $EO_{100}PO_{39}EO_{100}$ and $EO_{80}PO_{30}EO_{80}$, yield cubic mesoporous silica. Hexagonal mesoporous silica can also be synthesized by using reversed poly(alkylene oxide) triblock copolymer architectures, for example, $PO_{19}EO_{33}PO_{19}$. Ordered mesoporous silica can be prepared with more complicated surfactant architectures, for example, using star diblock copolymers, such as Tetronic 908 and Tetronic 901, and reversed star diblock copolymers, for example, Tetronic 90R4. We have obtained only cubic mesoporous silica structures with these star diblock copolymers. The BET surface areas, *d* spacing values, and pore sizes of the mesoporous silica phases (Table 2) do not have an obvious relationship to the length of the respective EO and PO groups. However, higher molecular weight block copolymers can be expected to give larger pore systems, and the upper limits of the accessible periodic pore structures are being investigated.

3. Hydrothermal Stability. One of the limitations of calcined MCM-41 materials prepared by using cationic surfactants without additional treatment with TEOS is their instability in water.[47−50] Both as-synthesized and calcined MCM-41, prepared by using $C_{16}H_{33}N(CH_3)_3Br$ as previously described, show well-resolved hexagonal XRD patterns (see Supporting Information Figure XII). However, after heating in boiling

(42) Wanka, G.; Hoffmann, H.; Ulbricht, W. *Macromolecules* **1994**, *27*, 4145.
(43) Luzzati, V.; Delacroix, H. Gulik, A. *J. Phys. II* **1996**, *6*, 405.
(44) Gulik, A.; Delacroix, H.; Kirschner, G.; Luzzati, V. *J. Phys. II* **1995**, *5*, 445.
(45) Kratzat, K.; Finkelmann, H. *Liq. Cryst.* **1993**, *13*, 691.
(46) Alexandridis, P.; Olsson, U.; Lindman, B. *Langmuir* **1997**, *13*, 23.
(47) Ryoo, R.; Jun, S. *J. Phys. Chem. B* **1997**, *101*, 317.
(48) Kim, J. M.; Kwak, J. H., Jim, S.; Ryoo, R. *J. Phys. Chem.* **1995**, *99*, 16742.
(49) Ryoo, R.; Kim, J. M.; Ko, C. H.; Shin, C. H. *J. Phys. Chem.* **1996**, *100*, 17718.
(50) Beck, J. C.; Chu, C. T.; Johanson, I. D.; Kresge, C. T.; Leonowicz, M. E.; Roth, W. J.; Vartuli, J. C.; McCullen, S. B. U.S. Patent 5,156,829, 1993.

water for 6 h, the structure of calcined MCM-41 is destroyed and the material becomes amorphous, as evidenced by the loss of all XRD scattering reflections. Ryoo et al. showed that the addition of salt, such as NaCl or EDTA, can improve the hydrothermal stability of MCM-41.[49] In contrast, all of the calcined samples studied in this paper prepared using the nonionic oligomeric surfactants or block copolymer surfactants are stable after heating in boiling water for at least 48 h under otherwise identical conditions. For example, for calcined SBA-15 prepared using $EO_{20}PO_{70}EO_{20}$ at 35 °C, after heating in boiling water for 6 h the (210) reflection becomes broader, the (300), (220), and (310) peaks become weaker, and the (100) peak is still observed with similar intensity. After heating in boiling water for 24 h, the intensity of the (100) Bragg peak remains unchanged with retention of the higher-order reflections. BET measurements carried out after such treatment show that the monodispersity of the pore size, surface area, and pore volume are retained. For example, if SBA-15 with a mean pore size of 60 Å, a BET surface area of 780 m^2/g, and a pore volume of 0.80 cm^3/g is treated in boiling water for 24 h, it then shows a mean pore size of 64 Å, a BET surface area of 690 m^2/g, and a pore volume of 0.79 cm^3/g. These results confirm that calcined SBA-15 is hydrothermally stable. SBA-15 has thicker silica walls than MCM-41, which appear to provide significantly improved thermal stability to the calcined materials in boiling water. This is an improved one-step alternative to two-step post-synthesis treatments that use TEOS to stabilize mesoporous MCM-41 by re-structuring the inorganic wall with additional silica.[24,50]

4. Formation of Mesoporous Silica. Pinnavaia et al.[8−10] used nonionic surfactants to synthesize disordered, wormlike mesoporous silica and alumina under neutral pH conditions, and proposed an S^0I^0 mechanism involving hydrogen-bonding interactions between the surfactant and siloxane species. In the present case, the mesoporous silica is formed in acid media (pH $\ll$ 1) by using acids such as HCl, HBr, HI, HNO_3, H_2SO_4, and even H_3PO_4 with Triton surfactants (see Experimental Section). Acetic acid is too weak (pH > 2.8). We have tried to use bases such as NaOH, $(CH_3)_4NOH$, $(CH_3CH_2O)_3N$, and $(CH_3)_3N$ as catalysts but failed to produce ordered materials with mesoporosity, obtaining only amorphous silica or silica gels. If the acid concentration is in the range of pH 2−6, no precipitation of silica is observed. In a neutral solution (pH ∼ 7), disordered mesoporous silica with a broad peak in the XRD pattern is obtained after calcination, in agreement with the observations reported by Pinnavaia et al.[8−10]

To examine the synthesis variables important to the formation of mesoporous silica in acid conditions, we measured the time required for silica mesophase precipitation, as a function of different acid anion and H^+ concentrations. The relative times required for precipitation to occur depend on the acid anion and follow the following sequence (from shorter to longer): HBr ∼ HCl < HI < HNO_3 < H_2SO_4 ≪ H_3PO_4 (Figure 10, top). The radius or charge of the anion and the strength of acid have a large effect on the reaction rates. As shown in Figure 10 (bottom), the time *t* needed before silica precipitation takes place decreases with increasing HCl concentration. Furthermore, for *C* equal to the concentration of hydrochloric acid, the plot of log(*t*) vs log(*C*) is linear with a slope of −0.62, the concentration of H^+ being equal to that of Cl^-. When the acid concentration is constant, the time required for mesophase silica precipitation decreases with increasing Cl^- concentration (produced by adding extra NaCl to the reaction solution), suggesting that the acid anion, Cl^-, is involved in the assembly of organic and inorganic

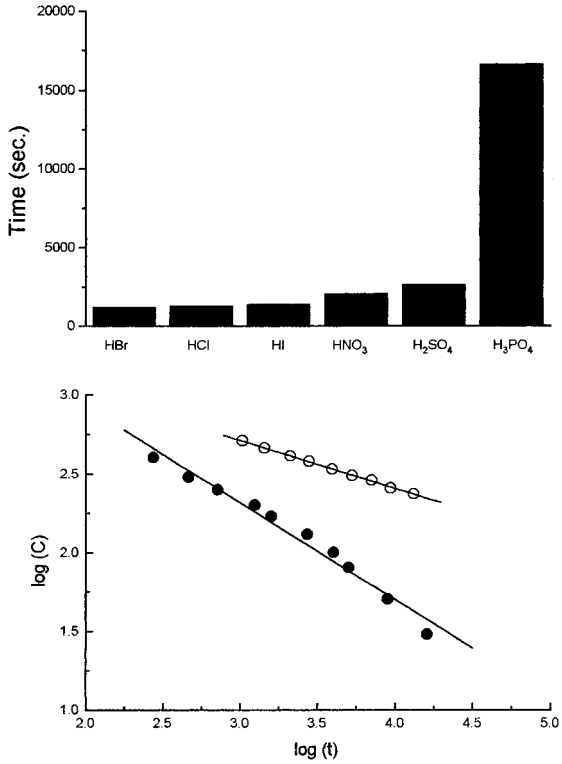

Figure 10. (Top) Time, *t*, when silica mesophases are precipitated from clear solution using different acids as catalysts. The reactions, with the composition of TEOS:Triton X100:A:H_2O (mol ratio) = 19.2: 1.55:100:4450, where A = HCl, HBr, HI, HNO_3, $^1/_2H_2SO_4$, or $^1/_3H_3PO_4$, were carried out at room temperature. (bottom) Plots of log(*t*) vs log(*C*), where *C* is the concentration of HCl (filled circles) and the concentration of additional Cl^- (open circles) for a fixed hydrogen ion concentration. The reaction compositions were similar to that given above, and the concentration of chloride was changed by adding extra NaCl.

mesophase products. The plot of log(*t*) vs log([Cl^-]) is linear with a slope of −0.31, half of −0.62. The results indicate that the rate (*r*) of mesophase silica precipitation with the structure-directing surfactant species can be described by $r = k[H^+]^{0.31}[Cl^-]^{0.31}$. We also note that when $C_{12}EO_4$ is used as the surfactant species, after a 3 h reaction at RT, lamellar mesostructured silica initially forms with *d*(100) of 49.9 Å and *d*(200) of 24.9 Å. However, after a 20 h reaction time, cubic SBA-14 results, suggesting that under these conditions mesostructured intermediates can be transformed into different mesophases as the extent of silica polymerization increases.[16,51]

On the basis of these results, we postulate that the assembly of the mesoporous silica organized by nonionic alkyl−ethylene oxide surfactants or poly(alkylene oxide) triblock copolymer species in acid media occurs through an $(S^0H^+)(X^-I^+)$ pathway.[20,35] First, alkoxysilane species are hydrolyzed

$$Si(OEt)_4 + nH_3O^+ \xrightarrow[pH < 2]{\text{hydrolysis}} Si(OEt)_{4-n}(OH_2^+)_n + n\text{EtOH}$$

which is followed by partial oligomerization at the silica. The EO moieties of the surfactant in strong acid media associating with hydronium ions

$$REO_m + yHX \xrightarrow{H_2O} REO_{m-y}[(EO)\cdot H_3O^+]_y\cdots yX^-$$

(51) Stucky, G. D.; Monnier, A.; Schüth, F.; Huo, Q.; Margolese, D.; Kumar, D.; Krishnamurty, M.; Petroff, P.; Firouzi, A.; Janicke, M.; Chmelka, B. F. *Mol. Cryst. Liq. Cryst.* **1994**, *240*, 187.

where R = alkyl or poly(propylene oxide) and $X^- = Cl^-$, Br^-, I^-, NO_3^-, $H_ySO_4^{-2+y}$, $H_yPO_4^{-3+y}$.

We propose that these charge-associated EO units and the cationic silica species are assembled together by a combination of electrostatic, hydrogen bonding, and van der Waals interactions $REO_{m-y}[(EO)\cdot H_3O^+]_y\cdots yX^-\cdots I^+$, which can be designated as $(S^0H^+)(X^-I^+)$. Coordination sphere expansion around the silicon atom by anion (e.g., Cl^-) coordination of the form $X^-\cdot Si-OH_2^+$ may play an important role.[20,35] During the hydrolysis and condensation of the silica species, intermediate mesophases, such as hexagonal, cubic, or lamellar mesostructures, are sometimes observed.[16,51] Further condensation of the silica species and organization of the surfactant and inorganic species result in the formation of the lowest energy silica−surfactant mesophase structure allowed by the solidifying inorganic network.[18,20,35]

Conclusion

Highly ordered, mesoporous silica structures have been synthesized by using commercially available nonionic alkylethylene oxide oligomeric surfactants and poly(alkylene oxide) block copolymer surfactants in strong acid media. The family includes materials with cubic cage structures *Im*$\bar{3}$*m*, cubic *Pm*$\bar{3}$*m* (or others), the three-dimensional hexagonal $P6_3/mmc$ cage structure, a honeycomb hexagonal *p*6*mm* structure, and lamellar (L_α) and possibly continuous L_3 sponge, mesophases. Under acidic conditions, nonionic alkyl−ethylene oxide oligomeric surfactants often favor the formation of cubic mesoporous silica phases at room temperature, while poly(alkylene oxide) triblock copolymers tend to favor the hexagonal (*p*6*mm*) mesoporous silica structure.

A cubic mesoporous silica phase (SBA-11) with a *Pm*$\bar{3}$*m* (or diffraction-related space group) structure has been synthesized in the presence of $C_{16}EO_{10}$ surfactant species. This material has a BET surface area of 1070 m^2/g and pore size of 25 Å. The three-dimensional hexagonal $P6_3/mmc$ mesoporous silica (SBA-12) phase can be synthesized by using $C_{18}EO_{10}$ surfactant species under otherwise similar conditions. Nonionic alkyl−EO/furan surfactants, such as Tween 60, can be used to form cubic mesoporous silica. Surfactants with shorter EO moieties form a less ordered material, which may be an L_3 sponge mesophase or a lamellar mesostructured silica. The former exhibits a BET surface area of 610 m^2/g and pore size of 24 Å, while the latter is thermally unstable to calcination. Hexagonal (*p*6*mm*) mesoporous silica with *d*(100) = 64−77 Å can be synthesized at 100 °C by using alkyl−ethylene oxide surfactants, such as $C_{16}EO_{10}$ and $C_{18}EO_{10}$.

Highly ordered hexagonal (*p*6*mm*) mesoporous silica SBA-15 with ultralarge *d*(100) spacings of 104−320 Å has been synthesized in the presence of poly(alkylene oxide) triblock copolymers, such as $EO_{20}PO_{70}EO_{20}$. SBA-15 has BET surface areas of 690−1040 m^2/g, large pore sizes of 46−300 Å, and unusually large pore volumes up to 2.5 cm^3/g, with silica wall thicknesses ranging from 31 to 64 Å. The pore size and silica wall thickness of SBA-15 are adjustable by varying the temperature (35−140 °C) and duration (11−72 h) of the reaction and by adding organic swelling agents, such as TMB. The organic structure-directing agents can be easily removed by heating at 140 °C for 3 h or by refluxing in EtOH.

A novel cubic (*Im*$\bar{3}$*m*) mesoporous silica with case structures (SBA-16) and a large cell parameter (*a* = 176 Å) has been synthesized by using poly(alkylene oxide) triblock copolymers with large EO group moieties, such as $EO_{106}PO_{70}EO_{106}$. SBA-16 has been prepared with a BET surface area of 740 m^2/g and a pore size of 54 Å. Star diblock poly(alkylene oxide) copolymers can also be used as structure-directing agents to form ordered cubic mesoporous silica phases. The EO/PO ratio of the copolymers has a large effect on the formation of the silica mesophase. Using triblock copolymers with smaller ratios (<0.07) such as $EO_5PO_{70}EO_5$, favors the formation of lamellar mesostructured silica, for example, with a *d*(100) spacing of 116 Å. A larger EO/PO ratio (>1.5) tends to favor the formation of cubic mesoporous silica structures. The calcined mesoporous silica structures reported in this paper are thermally stable in boiling water, probably related to the relatively thick silica walls. The hydrothermal stability decreases with increasing pore size, if achieved using cosolvent species such as TMB, consistent with the thinner silica walls that result. The assembly of the periodic inorganic and organic composite materials appears to occur by a hydrogen-bonding pathway involving cationic silica species that are present in the strong acid conditions.[20,35] As expected for $(S^0H^+)(X^-I^+)$ assembly, the assembly rate (*r*) increases with increasing concentration of H^+ and Cl^- and follows a rate law $r = k[H^+]^{0.31}[Cl^-]^{0.31}$.

Acknowledgment. We thank N. Melosh and Prof. G. H. Fredrickson for helpful discussions and BASF (Mt. Olive, NJ) for providing the block copolymer surfactants. Funds were provided by the National Science Foundation under Grants No. DMR 95-20971 (G.D.S.) and No. DMR 92-57064 (B.F.C.) and the U. S. Army Research Office under Grant No. DAAH04-96-1-0443. This work made use of MRL Central Facilities supported by the National Science Foundation under Award No. DMR-9632716. B.F.C. is a Camille and Henry Dreyfus Teacher-Scholar and an Alfred P. Sloan Research Fellow.

Supporting Information Available: Figures (12) showing experimental results: ^{29}Si NMR (one), XRD (four), BET isotherms (four), TEM images (two), TGA curve (one) (12 pages, point/PDF). See any current masthead page for ordering and Web access instructions.

JA974025I